High-Pressure Adsorption of Pure Coalbed Gases on Dry Coal Matrices

Arumugam, A.; Fitzgerald, J. E.; Sudibandriyo, M.; Robinson, Jr. R. L.; Gasem, K. A. M.

School of Chemical Engineering
Oklahoma State University
Stillwater, OK 74078

Abstract

As part of our efforts to model enhanced coalbed methane recovery and CO_2 sequestration in coalbeds, we have investigated the pure adsorption isotherm behavior of five dry coals namely, Illinois #6, Wyodak sub-bituminous, Pocahontas, Beulah Zap, and Upper Freeport coal. Using a volumetric technique, isotherms of pure methane, nitrogen, CO_2 and ethane were measured at a temperature of 328.15 K (131°F) and pressures to 13.8 MPa (2000 psia). In most cases, the adsorption replicate isotherms were measured to ascertain the experimental reproducibility. Errors from primary pressure, temperature, and volume measurements were propagated to estimate the uncertainty of each adsorption datum point. On average, the expected experimental uncertainty of the pure-gas adsorption data is 7%.

Ono-Kondo lattice model was used to represent the adsorption isotherms of the coals considered, and the model parameters were regressed for each coal. In general, the model represents the adsorption isotherms within their experimental uncertainties.

1. Introduction

Deep coalbeds retain large quantities of gases such as methane, nitrogen, and CO_2 through a phenomenon called adsorption. When a gas adheres to the surface of coal, the solid-gas interactions present can change the apparent gas density to that comparable to liquids. In coalbed reservoirs, methane resides inside the microporous coal structure at higher densities than the free gas phase due to physical adsorption. Gas species other than methane also reside in the coal seam: roughly 90% is methane, 8% carbon dioxide, 2% nitrogen, with traces of other hydrocarbons [1]. In U.S coalbeds alone, estimates predict that adsorptive processes hold about 135 trillion cubic feet of recoverable gas. This is approximately 14% of US natural gas reserves [2]. The implementation of coalbed methane technology accounted for 6% of the U.S. natural gas production in 1997 [3].

Currently, enhanced coalbed methane recovery (ECMR) processes utilize CO_2, nitrogen or mixtures of both gases to improve production rates. Specifically, nitrogen injections into CBM production wells are used to help displace methane gas [4]. By combining CO_2 with nitrogen, ECMR can displace more methane from coalbeds than with nitrogen alone [5]. Nitrogen injection raises the reservoir pressure to improve gas flow and displaces the adsorbed methane gas via stripping. In comparison, CO_2 injection selectively frees adsorbed methane gas from the coal because CO_2 equilibrium adsorption is greater than that of methane [4, 6]. CO_2 injection into coalbed reservoirs also may serve a sequestration function, which is a potential environmental benefit.

To assess the economic and environmental potential of CBM operations, an experimental database of high-pressure gas adsorption on coals is sought to determine the relative adsorption affinities of various gases on coals. Most of our past gas adsorption measurements have been performed exclusively on water-moistened coal to represent better *in-situ* coalbed conditions. To assess the effect of water on gas adsorption, our goal is to measure the pure gas adsorption on various coals, both in a water-moistened and dry state; this work concerns the latter. Measurements of methane, nitrogen, CO_2, and ethane adsorption on five dry coals from the Argonne National Laboratory were studied. Hysteresis and repeat measurements were performed to investigate the gas adsorption reproducibility. The measurements were modeled with the Ono-Kondo model.

2. Experimental Apparatus and Void Volume Measurements

The experimental method used in the OSU adsorption laboratory is based on a mass balance principle, which employs precise measurements of pressures, volumes and temperatures. The experimental apparatus, shown schematically in Figure 1, has been used successfully in previous studies [7, 8]. The pump and cell sections of the apparatus are maintained in a constant temperature air bath at a pre-determined temperature. For this study all measurements are performed at 131°F (328.2K). The equilibrium cell has a volume of 110 cm^3 and is filled with the adsorbent to be studied. The cell is placed under vacuum prior to gas injection. The void volume, V_{void}, in the equilibrium cell is then determined by injecting known quantities of helium from a calibrated injection pump (Ruska Pump). Since helium is not significantly adsorbed, the void volume can be determined from measured values of

temperature, pressure and amount of helium injected into the cell. Several injections made into the cell at different pressures show consistency in the calculated void volume. Generally, the void volume calculated from sequential injections varies less than 0.3 cm^3 from the average value (of approximately 100 cm^3).
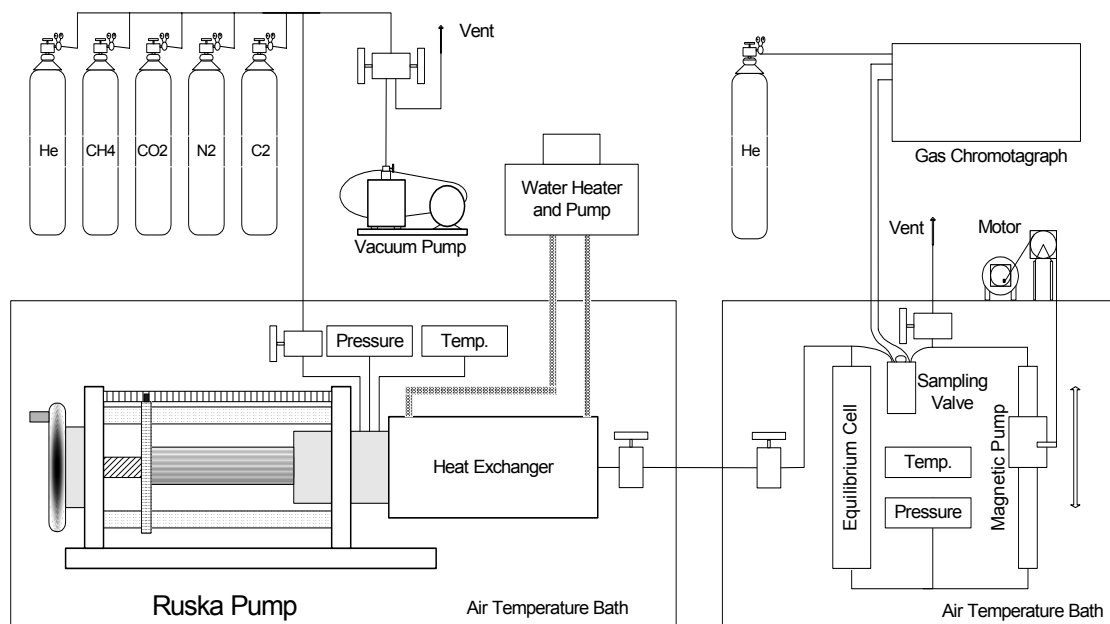

Figure 1. Schematic Diagram of the Experimental Apparatus

A mole balance and use of the real gas law allows calculation of the helium void volume:

$$V_{void} = \frac{\left(\dfrac{P\Delta V}{ZT}\right)_{pump}}{\left(\dfrac{P_1}{Z_1 T} - \dfrac{P_2}{Z_2 T}\right)_{cell}} \tag{1}$$

For void volume determination, the compressibility of helium is given by

$$Z_{He} = 1 + \left(0.001471 - 0.000004779\,T + 0.00000000492\,T^2\right)/P, \tag{2}$$

where T is in Kelvin and P is in atmospheres. This expression was obtained from Hall [8].

3. Pure-Gas Adsorption Measurements

The excess adsorption can be calculated directly from experimental quantities. For pure-gas adsorption measurements, a known quantity, n_{inj}, of gas (e.g., methane) is injected from the pump section into the cell section. Some of the injected gas, n_{inj}, will be adsorbed.

Although the amount of unadsorbed gas cannot be always inferred, the gas amount occupying the void volume, n_{unads}^{Gibbs}, can be inferred, and it is used to calculate the excess adsorption. A molar balance is used to calculate the excess amount adsorbed as

$$n^{Ex} = n_{inj} - n_{unads}^{Gibbs} \qquad (3)$$

The amount injected can be determined from pressure, temperature and volume measurements of the pump section:

$$n_{inj} = \left(\frac{P\Delta V}{ZRT}\right)_{pump} \qquad (4)$$

The unadsorbed amount of gas is inferred at the final equilibrium pressure. The void volume is assumed to remain constant for all pressures.

$$n_{unads}^{Gibbs} = \left(\frac{P}{ZRT}\right)_{cell} V_{Void}^{He} \qquad (5)$$

As indicated by equations (4) and (5), gas-phase compressibility (Z) factors are required for methane, nitrogen, CO_2, and ethane to analyze the experimental data. The compressibility factors for pure methane, nitrogen, CO_2, and ethane were determined from highly accurate equations of state [9-12].

The coals were dried under vacuum in an equilibrium cell at 353 K for 36 hours before being used in the adsorption measurements [1]. The mass of the coal sample was weighed (while still under vacuum in the equilibrium cell) after the drying. An ultimate and proximate analysis was performed for each coal by Argonne National Laboratory and is provided in the table below.

Table 1. Compositional Analysis of Coals from Argonne National Laboratory

Analysis*	Beulah Zap	Wyodak	Illinois #6	Upper Freeport	Pocahontas
Ultimate					
Carbon %	72.9	75.0	77.7	85.5	91.1
Hydrogen %	4.83	5.35	5.00	4.70	4.44
Oxygen %	20.3	18.0	13.5	7.5	2.5
Sulfur %	0.80	0.63	4.83	2.32	0.66
Ash %	9.7	8.8	15.5	13.2	4.8
Proximate					
Moisture %	32.2	28.1	8.0	1.1	0.7
Vol. Matter %	30.5	32.2	36.9	27. 1	18.5
Fixed Carbon %	30.7	33.0	40.9	58.7	76.1
Ash %	6.6	6.3	14.3	13.0	4.7

4. Ono-Kondo Adsorption Model

An adsorption model based on the lattice theory was proposed first by Ono and Kondo in 1960 [13]. The more general formalism was recently developed further by Donohue and coworkers for the adsorption of solutes in liquid solutions [14-17]. In the lattice model, the fluid system is assumed to be composed of layers of lattice cells that contain fluid molecules and vacancies.

Benard and Chahine [18] assume that the adsorption process is directly mapped on the two parallel hexagonal graphite planes. Figure 2 shows the adsorbed molecules inside the slit, and Figure 3 shows the adsorbed molecules positioned among the carbon atoms of the graphite planes. In this approach, the equilibrium equation becomes:

$$\ln[x_{ads}(1-x_b)/x_b(1-x_{ads})] + ((z_1+1)x_{ads} - z_0 x_b)\varepsilon_{ii}/kT + \varepsilon_{is}/kT = 0 \qquad (6)$$

where $z_1 = 6$ and $z_0 = 8$ for the hexagonal lattice cell. The interaction energy between molecule i and j is expressed by ε_{ij}, and ε_{is} is the interaction energy between molecule i and the solid surface.
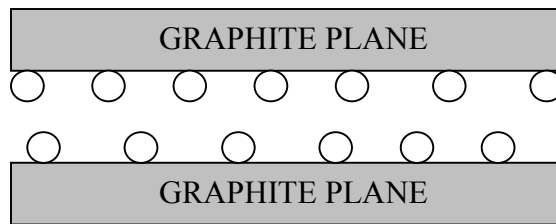

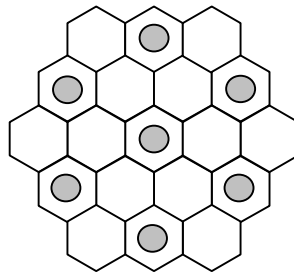**Figure 2. Monolayer Adsorption on Graphite Slit**

**Figure 3. Adsorbed Molecules Positioned among the
Carbon Atoms of the Graphite Planes**

According to the lattice theory, the excess adsorption is defined as

$$n_i^{Ex} = C_i \sum_{t=1}^{m} (x_{i,t} - x_{i,b})$$

(7)

where $x_{i,t}$ is the fraction of adsorbed molecules i that occupy the lattice cells at layer t ($= N_{i,t}/M_t$), and $x_{i,b}$ is the fraction of gas molecules i occupying the same number lattice cells as those at layer t ($= N_{i,b}/M_t$). This fractional coverage can also be expressed as $x_{i,t} = \rho_{i,t}/\rho_{i,mc}$ and $x_{i,b} = \rho_{i,b,}$ /•$\rho_{i,mc}$, where $\rho_{i,t}$ is the adsorbed density of component i at layer t, $\rho_{i,b}$ is the gas density of component i, and $\rho_{i,mc}$ is the adsorbed density of component i at the maximum capacity. The prefactor C_i represents the maximum capacity of the adsorbent. For pure adsorption inside the slit, according to the approach by Benard and Chahine, the number of layers, *m,* is equal to two, and equation (7) becomes:

$$n^{Ex} = 2C \ (x_{ads} - x_b) = 2C \left(\frac{\rho_{ads}}{\rho_{mc}} - \frac{\rho_b}{\rho_{mc}} \right)$$

(8)

Here, the pre-factor C may be assumed to be a parameter taking into account the fraction of the active pores of the adsorbent and other structural properties of the adsorbent. C/ρ_{mc} represents the specific adsorbed-phase volume for the adsorbate-adsorbent system.

Equation (6) is used for monolayer adsorption equilibrium, and together with equation (8) they can be used to correlate the experimental excess adsorption isotherm to obtain four parameters per gas, i.e., ε_{ii}/k, ε_{is}/k, ρ_{mc} and C. These four parameters are optimized using the following objective function:

$$OBJ = \sum_{i}^{npts} ((n_{i,calc}^{Ex} - n_i^{Ex})/\sigma_i)^2$$

(9)

where σ_i is the expected uncertainty for point i.

5. Results and Discussions

Figures 4-8 depict adsorption for the four gases on all of the five coals. The excess adsorption depicted is *not* on an ash-free basis, but rather on a dry-coal mass basis. All Ono-Kondo model regressions fit each isotherm well within the experimental uncertainties, on average.

In the figures, error bars represent the expected uncertainty for the experimental adsorption. The size of the uncertainty was determined by propagating errors from primary pressure, temperature, and volume measurements to the inferred excess adsorption quantity. In general, the average expected experimental uncertainty of the pure-gas adsorption data is about 7%. Uncertainties are smallest for nitrogen and largest for ethane. Ethane is the most compressible gas; thus, its gas density is more sensitive to small pressure and temperature

errors. In contrast, nitrogen has a compressibility factor close to 1.0 for all pressures, which produces smaller error bars.

The gas adsorption isotherms on all the coals have some general characteristics. Specifically, at low pressures, an amount of adsorbed gas is observed to be increasing in the following order: nitrogen, methane, ethane, and CO_2. Ethane isotherms have excess adsorption maximums between 4 to 6 MPa and CO_2 isotherms have excess adsorption maximums between 6 to 8.5 MPa.

Figures 9-12 depict the excess adsorption of each gas for all the five coals. The excess adsorption of methane between any of the coals varies by no more than 35% at pressures from 10 to 14 MPa; nevertheless, qualitative differences in the isotherm shape are apparent. The excess adsorption isotherm of methane on Upper Freeport and Pocahontas appears flat at pressures higher than 10 MPa. Methane adsorption on the other coals is increasing slightly with pressure at 10 MPa. The apparent order in the amount of methane adsorbed among the coals is Pocahontas, Illinois #6, Wyodak, Beulah Zap, and Upper Freeport. Nitrogen adsorption varied by no more than 45% in the amount adsorbed between any of the coals at pressures of 10 to 14 MPa. The apparent order in the amount of nitrogen adsorbed among the coals is Pocahontas, Wyodak and Illinois #6 (tied), and Upper Freeport and Beulah Zap (tied).

The apparent order in the amount of CO_2 adsorbed among the coals is Wyodak, Beulah Zap, Illinois #6, Pocahontas, and Upper Freeport. The CO_2 adsorption on Wyodak and Beulah Zap are almost indistinguishable until 10 MPa. These two coals have similar ultimate and proximate analyses. At the excess adsorption maximum, the excess adsorption of both CO_2 and ethane varies by no more than 110% between any of the coals.

Ethane adsorption exhibits unique features on some of the coals. Adsorption isotherms on Wyodak and Beulah Zap have a *minimum* after the adsorption maximum. These features, however, are suspect due to measurement uncertainty.

The ratio of CO_2 to ethane adsorption at different pressures varies notably among the coals. Beulah Zap has the largest ratio, with Wyodak close behind. Pocahontas has the smallest ratio. The CO_2/ethane adsorption ratio appears to increase qualitatively with the natural equilibrium moisture content of the coal, or decrease qualitatively with oxygen content.

Figures 13-15 depict measurements of methane adsorption on (a) a fresh coal matrix, (b) methane adsorption after CO_2 adsorption, and (c) methane adsorption after both CO_2 and ethane adsorption. Little, if any, variation in isotherm reproducibility is shown. The methane adsorption isotherm on Pocahontas is slightly outside expected uncertainties for some pressures after CO_2 adsorption. The methane adsorption after CO_2 and ethane adsorption, however, is identical (within the experimental uncertainty) to the methane adsorption on the fresh matrix.
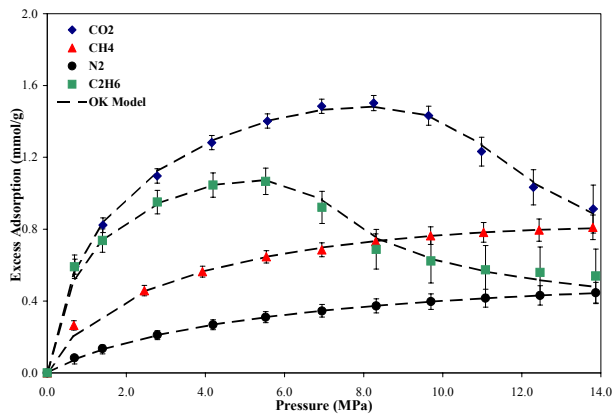
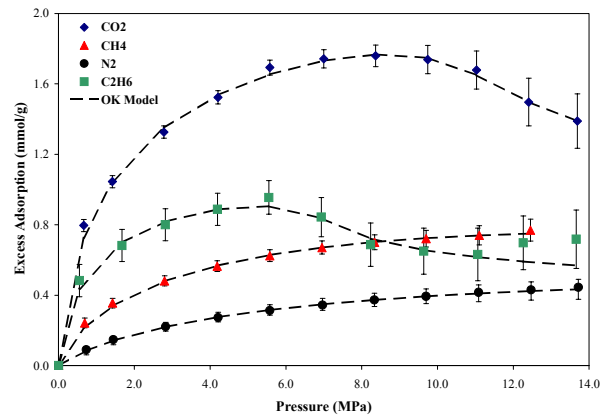**Figure 4: Adsorption of Pure Coalbed Gases on Dry Illinois #6 Coal at 328 K**

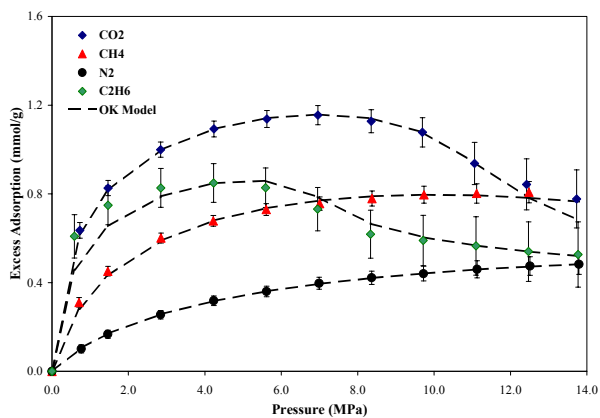**Figure 5: Adsorption of Pure Coalbed Gases on Dry Wyodak Coal at 328 K**

Figure 6: Adsorption of Pure Coalbed Gases on Dry Pocahontas Coal at 328 K
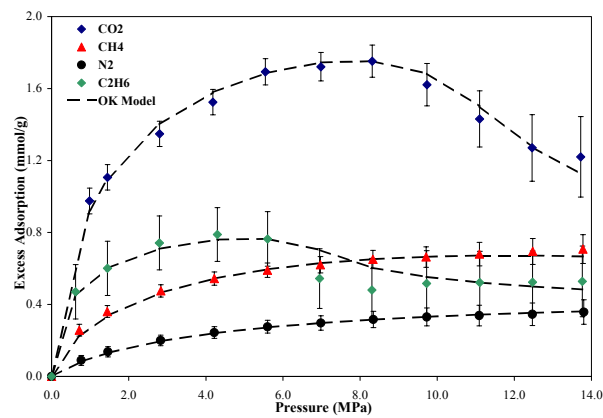

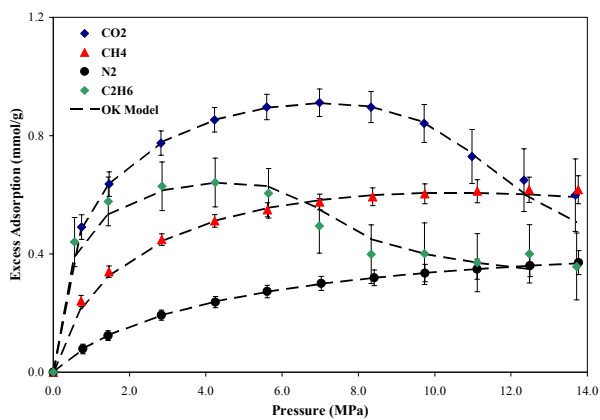**Figure 7: Adsorption of Pure Coalbed Gases on Dry Beulah-Zap Coal at 328 K**

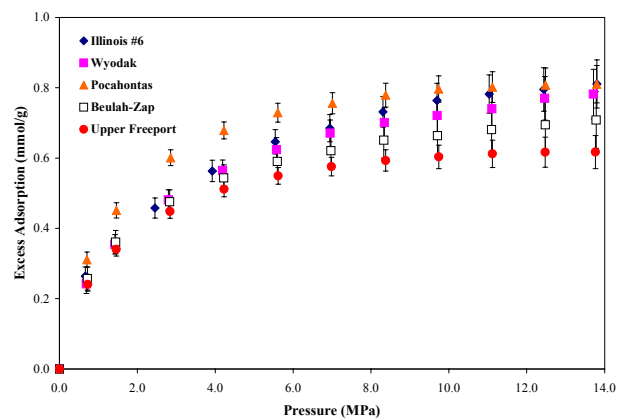**Figure 8: Adsorption of Pure Coalbed Gases on Dry Upper Freeport Coal at 328 K**

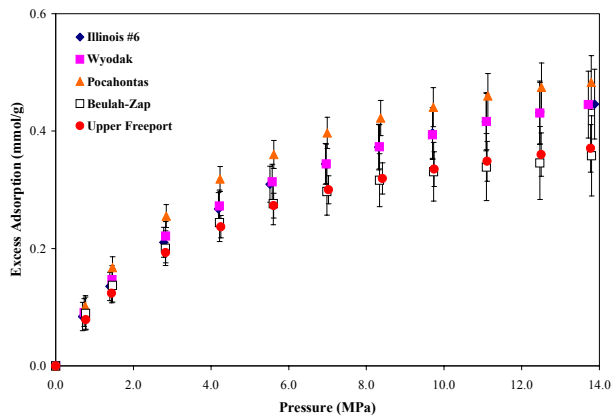**Figure 9: Adsorption of Pure Methane on Different Dry Coal Matrices at 328 K**

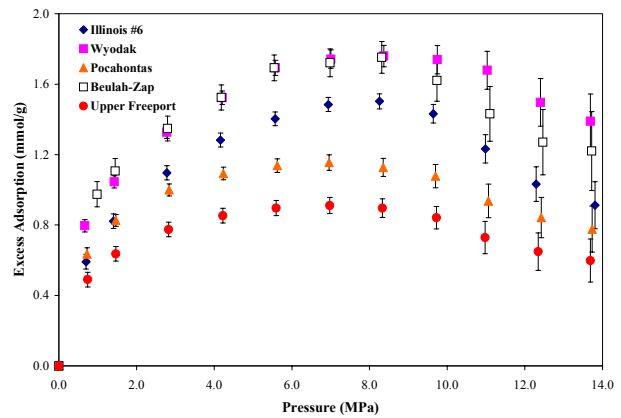**Figure 10: Adsorption of Pure Nitrogen on Different Dry Coal Matrices at 328 K**

Figure 11: Adsorption of Pure CO_2 on Different Dry Coal Matrices at 328 K
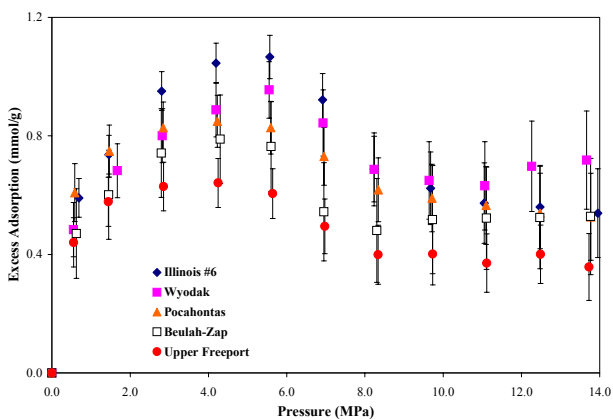

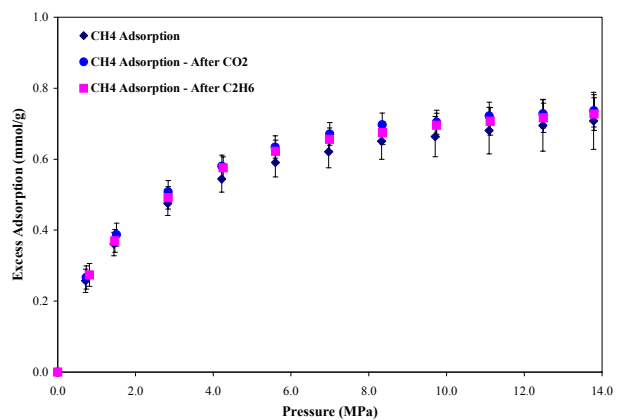**Figure 12: Adsorption of Pure Ethane on Different Dry Coal Matrices at 328 K**

Figure 13: Adsorption of Pure Methane on Beulah Zap before and after CO_2 and Ethane Gas Adsorption at 328 K
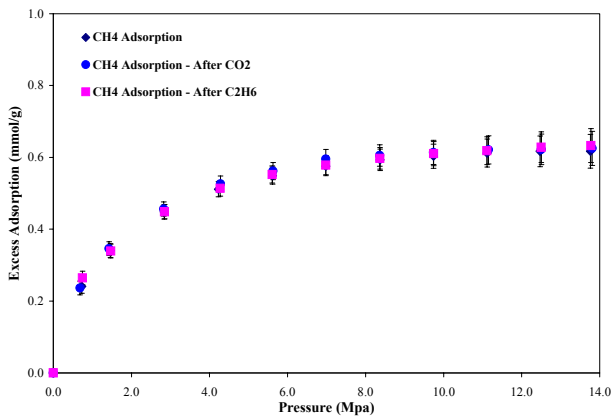

Figure 14: Adsorption of Pure Methane on Upper Freeport before and after CO_2 and Ethane Gas Adsorption at 328 K
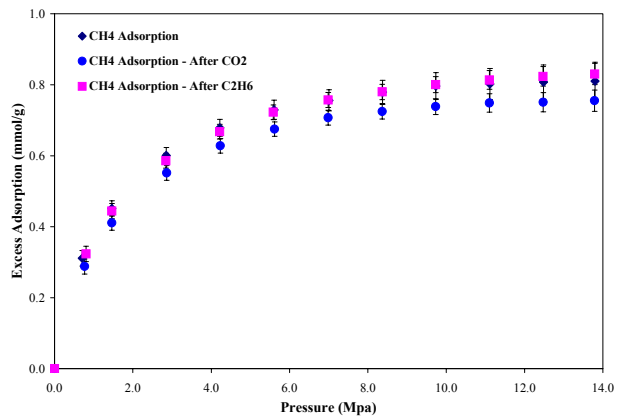

Figure 15: Adsorption of Pure Methane on Pocahontas before and after CO_2 and Ethane Gas Adsorption at 328 K

6. Conclusions

We have investigated the pure adsorption isotherm behavior of five dry coals namely, Illinois #6, Wyodak, Pocahontas, Beulah Zap, and Upper Freeport coal. Methane, nitrogen, CO_2 and ethane gas adsorption were measured at 328.15 K and pressures to 13.8 MPa. These newly acquired data constitute a valuable addition to the literature high-pressure adsorption data.

Methane and nitrogen showed far less variation in adsorption amounts than either CO_2 or ethane. The ratio of CO_2 to ethane adsorption varies notably among the coals. Little, if any, variation in isotherm reproducibility is shown for methane after the coal has been subjected to CO_2 and ethane gas adsorption.

The Ono-Kondo model is capable of representing precisely each isotherm within the experimental uncertainties.

7. References

1. Gasem, K.A.M., Robinson, Jr., R.L., Sudibandriyo, M., Pan, Z., Fitzgerald, J.E., *CO_2 Adsorption on Selected Coals*, Prepared for The Department of Energy - National Energy Technology Laboratory (NETL), (2003).
2. Mavor M., Pratt T., DeBruyn R. *Study Quantifies Powder River Coal Seam Properties,* Oil and Gas Journal, 35-50, April 26 1999.
3. Mavor M., Pratt T., Nelson C.R. *Quantitative Evaluation of Coal Seam Gas Content Estimate Accuracy*, SPE Paper 29577 (1995).
4. Stevens S.H., Spector D., Riemer P. *Enhanced Coalbed Methane Recovery Using CO_2 Injection: Worldwide Resource and CO_2 Sequestration Potential*, 1998 SPE International Conference in China, Beijing, China, November 1998.
5. Arri L.E., Yee D., Morgan W.D., Jeansome M.W. *Modeling Coalbed Methane Production with Binary Gas Adsorption*. SPE Paper 24363 (1992).
6. Stevens S., Spector D., Reimer P. SPE 48881. *Enhanced Coalbed Methane Recovery Using CO2 Injection: Worldwide Resource and CO2 sequestration Potential*, Proceedings, Sixth International Oil and Gas Conference and Exhibition in China, Vol. 1, November 1998.
7. Gunter W.D., Gentzis T., Rottenfusser B.A., Richardson R.J.H. *Deep Coalbed Methane in Alberta, Canada*. Energy Conversion Management; <u>38</u> suppl. S217-S222, (1997).
8. Hall, F., Zhou, C., Gasem, K.A.M., Robinson, Jr., R.L., *Adsorption of Pure Methane, Nitrogen, and Carbon Dioxide and Their Binary Mixtures on Wet Fruitland Coal*, presented at the Eastern Regional Conference & Exhibition, Charleston, November 8-10, 1994.
9. Sudibandriyo, M., Pan, Z., Fitzgerald, J.E., Robinson, Jr., R.L., Gasem, K.A.M., *Adsorption of Methane, Nitrogen, Carbon Dioxide and their Binary Mixtures on Dry Activated Carbon at 318.2 K and Pressures to 13.6 MPa*, Langmuir <u>19</u> (13), 5323-5331 (2003).
10. Angus, S., Armstrong, B., de Reuck, K.M*., International Thermodynamic Tables of the Fluid State-5: Methane*, IUPAC Chemical Data Series <u>16</u>, Pergamon Press, New York (1978).
11. Angus, S., de Reuck, K.M., Armstrong, B., *International Thermodynamic Tables of the Fluid State-6: Nitrogen*, IUPAC Chemical Data Series <u>20</u>, Pergamon Press, New York, (1979).
12. Span, R.,Wagner; W., *A New Equation of State for Carbon Dioxide Covering the Fluid Region from the Triple Point Temperature to 1100 K at Pressures up to 800 MPa*, J. Phys. Chem. Ref. Data, <u>25</u> 1509-1590 (1996).
13. Friend, D.G.; Ingham, H.; Ely, J.F., *Thermophysical properties of ethane*, J. Phys. Chem. Ref. Data, <u>20</u> (2), 275-347 (1991).
14. Ono, S., Kondo, S., *Molecular Theory of Surface Tension in Liquids*, in "Encyclopedia of Physics (S. Flugge, Ed.), Vol. X.," Springer-Verlag, Gottingen, (1960).
15. Aranovich, G.L., Donohue, M.D., *Adsorption of Supercritical Fluids*, J. Colloid and Interface Sci. <u>180</u> 537-541 (1996).
16. Aranovich, G.L., Donohue, M.D., *Predictions of Multilayer Adsorption Using Lattice Theory*, J. Colloid and Interface Sci. <u>189</u> 101-108 (1997).

17. Hocker, T., Aranovich, G.L., Donohue, M.D., *Monolayer Adsorption for the Subcritical Lattice Gas and Partially Miscible Binary Mixture*, J. Colloid and Interface Sci. <u>211</u> 61-80 (1999).
18. Hocker, T., Aranovich, G.L., Donohue, M.D., *Monolayer Adsorption of Nonrandom Mixtures*, J. Chem. Phys. <u>111</u> (3) 1240-1254 (1999).
19. Benard, P., Chahine, R., *Modeling of High-Pressure Adsorption Isotherms above the Critical Temperature on Microporous Adsorbents: Application to Methane,* Langmuir, <u>13</u> 808-813 (1997).